International Conference on Nuclear Data for Science and Technology 2007
DOI: 10.1051/ndata:07274

Fine structure in the intermediate resonance region of the neutron induced fission cross section

M. Mirea[1,a] and L. Tassan-Got[2]

[1] Institute of Physics and Nuclear Engineering, 077125 Bucarest, Romania
[2] Institut de Physique Nucléaire, 91406 Orsay Cedex, France

Abstract. Recently, the fine structure of the 0.7 MeV resonance in the ^{230}Th neutron-induced cross section was investigated within the hybrid model. A very good agreement with experimental data is obtained. It is suggested that fine structure of the cross section quantify the changes of the intrinsic states of the nucleus during the disintegration process. Due to internal excitations produced in the region of the outer barrier, where the density of single-particle states is enhanced, new transitions levels are produced. These transitions levels cause β-resonances very close in energy. A way to introduce phenomenologically this phenomenon in cross section calculations is presented.

1 Introduction

An early experimental data analysis of the 0.7 MeV resonance of the ^{230}Th neutron induced fission cross section evidences a high moment of inertia of the rotational band associated to this peak [1]. Intuitively, a such behavior indicates the possible existence of an intermediate state at a deformation energy considerably larger than that of the second minimum. A third minimum hypothesis was confirmed in refs. [2–4]. The fine structure of the 0.7 MeV resonance investigated in terms of the rotational model with two $\Omega = 1/2$ band heads of opposite parities revealed a moment of inertia parameter $\hbar^2/2J$ of about 1.9 keV. This value is considered compatible with the third minimum.

2 The hybrid model

A new model for intermediate resonance structures in the neutron-induced fission cross section was published recently [5]. The hybrid model employs phenomenological heights of the double humped barrier while the nuclear excitations are given by theoretical dynamical calculations. The deformation energy surface is determined in the framework of the microscopic-macroscopic model in a configuration space spanned by the most important degrees of freedom encountered in fission: elongation, necking and mass-asymmetry. The macroscopic energy is obtained with the Yukawa-plus-exponential model while the shell correction with the Strutinsky prescriptions based on the super-asymmetric two centers shell model [6]. A minimal action trajectory is determined in this configuration space in order to determine the shape of the barrier. Dynamical calculations are performed using the Landau-Zener effect in order to determine the occupation probability of each orbital in the path from the fundamental state up to scission. The occupation probabilities and the associated single-particle levels are afterwards translated in excitations of the barrier. These excitations are added to a phenomenological barrier. A great number of double barriers are obtained, each of them represents a transition level and it is characterized by a probability of realization. Each barrier gives rise to beta resonance in the second well together within the associated sequence of rotational resonances. These resonances are characterized by a spin quantum number. The weighted convolution of these resonances gives the intermediate structure.

The fine structure of the 0.7 MeV resonance of the neutron-induced fission cross section of ^{230}Th was attacked within this model [7]. An excellent agreement with experimental data was obtained. It was shown that the fine structure can be explained by the promotion of the unpaired nucleon from one single-particle level to another in the region of the second barrier, where the density of levels is very large. The probability that a nucleon skips from a level to another in the avoided crossing regions is amplified in the vicinity of the outer barrier. A way to introduce the single-particle effects evidenced by the new formalism in the phenomenological evaluations will be drawn.

The neutron single-particle level scheme is plotted in figure 1(a). For elongations comprised between $R = 0$ (spherical shape) and the R $\approx$ 7 fm (fundamental state) the shapes are considered symmetrical by reflection, therefore the parity and the intrinsic spin projection Ω are good quantum numbers. From R $\approx$ 7 fm up to the scission, the system loses the reflection symmetry to reach the final partition with ^{131}Sn heavy fragment and the parity is no longer a good quantum number. Therefore, single-particle interactions can be produced easily between levels characterized by the same value of Ω. The spin interaction constants were choose to reproduce as well as possible the experimental sequence of the first excited levels in the ^{231}Th. Excepting the $5/2^-$ bandhead, the first single-particle excited states are retrieved for $R \approx 7$ fm: $5/2^+$ (fundamental level), followed by the $3/2^+$ and $1/2^+$ excited states. The fundamental state is considered in the present work to have reflection-symmetry. If reflection-asymmetry or mass-asymmetry is considered, the system acquires a doublet structure containing both parities of Ω, and the $5/2^-$ bandhead will naturally appear in the sequence of levels. For the ^{231}Th compound nucleus, the lowest lying fission channels are essentially low-Ω single-particle states. Higher spins are not allowed by the compound nucleus formation cross section

[a] Presenting author, e-mail: mirea@ifin.nipne.ro

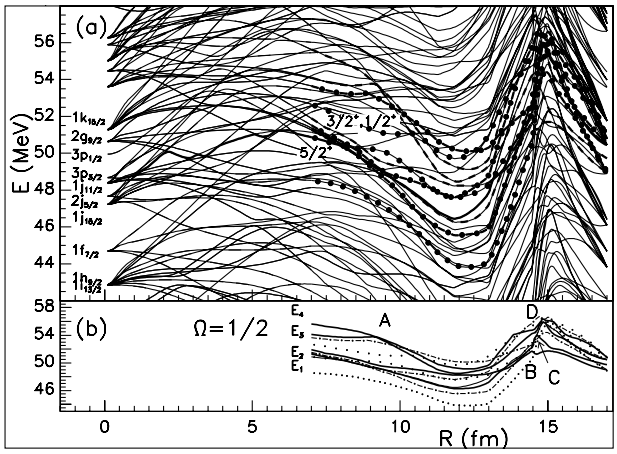

Fig. 1. (a) Neutron level scheme as function of the elongation. For zero elongation ($R = 0$), the shape parameterization describes a spherical nucleus. For low values of the deformations, the system behaves as a Nilsson level scheme. Asymptotically ($R \to \infty$), the two level schemes of the formed fragments are superimposed. The last occupied level is plotted with a thick full line. Levels of interest are also plotted with different thick line types: dashed line for four $\Omega = 1/2$ levels, dashed-dotted line for three $\Omega = 3/2$ levels, dotted lines for two levels of spin projection 5/2 and one of 7/2. The Nilsson parameters κ and μ are 0.0637 and 0.74, respectively. (b) The four adiabatic $\Omega = 1/2$ interesting levels are displayed with full thick lines and numbered. The selected avoided crossing regions between $\Omega = 1/2$ levels are marked with letters. The other selected levels and the last occupied one are displayed with narrow lines of same types as in plot (a). Figure from ref. [6].

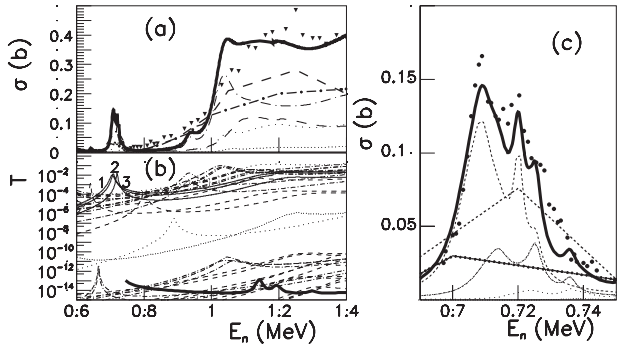

Fig. 2. (a) Cross section in the threshold region with respect to the neutron energy determined in the frame of hybrid model compared with ENDF/B-VI.8 and JENDF-3.3 [10] evaluations (thick dot-dashed and dashed lines, respectively). Experimental data extracted from ref. [1] are also presented as down-point triangles. The partial contributions in the cross section of different spins of the compound nucleus are displayed with dashed lines for $I = 1/2$ (I spin of the compound nucleus), dot-dashed lines for 3/2 and dotted lines for 5/2 and 7/2. (b) Weighted transmissions of the excited barriers that contribute to the total cross section. Same line types are used as in the plot (a) excepting the three transmissions corresponding to barriers 1, 2 and 3 where a full line is used. (c) Detailed representation of the cross section in the region 0.7 MeV. The spin dependent partial cross sections are also given. The ENDF and JENDF evaluations are plotted with dot-dashed and dashed lines, respectively. Experimental data from ref. [2] are also given as full points. Figure from ref. [6].

at low energy. Several single-particle levels that lie close to the adiabatic last occupied level are selected as displayed in figure 1(b). The single-particle levels with the same good quantum numbers associated with some symmetries of the system cannot in general intersect but exhibit avoided level crossings [8]. Our system being characterized by an axial symmetry, the good quantum numbers are the intrinsic spin projections Ω. The radial coupling causes transitions of the unpaired nucleon from one level to another of same Ω. The probability to jump from one level to another can be evaluated by quantifying the Landau-Zener effect with a system of microscopic equations of motion as realized in ref. [9]. Solving the coupled channel equations system, the amplitudes of the single-particle wave functions in the nuclear level distribution is determined. In this way, the probability of occupation of an excited level is obtained.

For the four $\Omega = 1/2$ levels, four avoided crossing regions are selected, marked with letters A, B, C and D on the figure 1(b). If the unpaired nucleon is initially located on the level E_1, it can follow during the disintegration any of the following paths E_2BE_1, E_2BCE_2, E_2BCDE_3 or E_2BCDE_4 opened by the avoided crossing regions B, C and D. If the unpaired neutron is initially located on another excited level, different energy paths are open. 18 different excitation channels can be obtained within the selected configuration of only four levels and four avoided crossing regions. In the case of the three $\Omega = 3/2$ selected levels, in a similar manner, 13 different additional excitations are obtained.

The theoretical excitations computed in the frame of the superfluid model are added to a phenomenological barrier. The mixing is realized in the most simplest way by realizing a linear interpolation based on a correspondence between some points (R, ε). R is the elongation for the theoretical model and ε the dimensionless parameter used in simulating the phenomenological barrier. The correspondence was choose for the two minima, the two heights and the exit point. The hybrid model emerges. New barriers are constructed. An imaginary component of the potential is considered in the second well to take into account other de-excitation channels apart the fission one. The magnitude of this imaginary component increases with the excitation energy of the compound nucleus and it is computed with the recipe of ref. [5]. Finally, the barriers associated to the excitations and their weights are used to determine the cross section by invoking the detailed balance principle. Results are plotted in figure 2 for the following heights and stiffnesses of the phenomenological barrier: $V_A = 6.24\,\text{MeV}$, $V_{II} = 2.37\,\text{MeV}$, $V_B = 6.29\,\text{MeV}$, $\hbar\omega_A = 0.65\,\text{MeV}$, $\hbar\omega_{II} = 1\,\text{MeV}$ and $\hbar\omega_B = 1.37\,\text{MeV}$. In the region [0.7, 0.75] MeV a fine structure is found by the simulation that agrees very well with experimental data as evidenced in figure 2(c). Unfortunately, the increasing flank of the cross section around 1 MeV is not well reproduced. Other parameters of the phenomenological barrier succeed to reproduce better this region of the cross section but in the same time lead to a degradation of the quality, for reproducing the cross section behavior around 0.7 MeV. The main question concerns the origin of these fine structure resonances at 0.7 MeV. This structure is produced by very close β-resonances of three excited single-particle barriers of spin 1/2 superimposed on resonances due to rotations of the core. The barriers with excitations created by the opened single-particle energy paths E_2BCE_2, E_2BCDE_3 and E_2BCDE_4. In the vicinity of the top

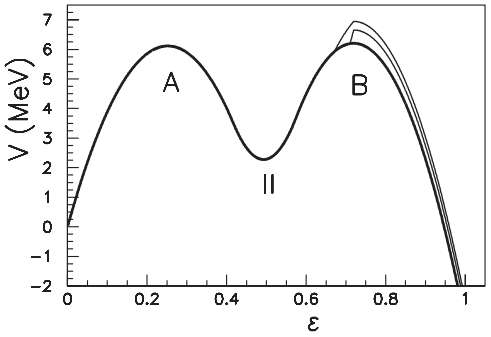

Fig. 3. Phenomenological barrier with possible excitations from a transition level to another in the region of the outer hump.

of the second barrier, (the elongation being R ≈ 15 fm) a very large density of levels is revealed. This behavior creates premises for an increased number of avoided crossing levels regions and, therefore, for a similar number of small single-particle excitations. The unpaired neutron on the adiabatic level E_2 has a finite probability to jump on the level E_3 at point C and, successively, on the level E_4 at point D (see fig. 1(b)). Three excited barriers of interest can be obtained in this way. The three excited barriers are different only in a small interval around the top of the outer barrier up to the exit point, and therefore give three different β-resonance very close in energy. These resonances are plotted and marked in figure 2(b) with their respective numbers 1, 2 and 3. These three resonances are in an energy interval smaller than 0.05 MeV and produce three main fine peaks in the fission cross section. Rotational resonances are constructed on these $\Omega = 1/2$ members leading to additional structures. The structure due to rotations can be identified by analyzing the figure 2(c) where the role played by partial cross sections of spin 3/2, 5/2 and 7/2 can be acknowledged.

3 Phenomenological approximation

Landau and Zener provided a simple formula to determine the probability P that an unpaired nucleon jumps from an adiabatic level ϵ_1 to another ϵ_2 in an avoided crossing region:

$$P = \exp\left(-\frac{2\pi\Delta\epsilon^2}{\hbar \mathrm{d}\left|\epsilon_1 - \epsilon_2\right| / \mathrm{d}t}\right), \tag{1}$$

where $\Delta\epsilon$ is the matrix element of the residual interaction between the two levels. For a reaction time included in the interval $[10^{-21}, 10^{-20}]$ s, the internuclear velocity between the nascent fragments is estimated $\mathrm{d}R/\mathrm{d}t \subset [1.5 \times 10^6, 1.5 \times 10^7]$ fm/fs. With a slope $\mathrm{d}|\epsilon_1 - \epsilon_2|/\mathrm{d}R \subset [0.5, 4]$ MeV/fm, and a residual interaction $\Delta\epsilon \subset [0.1, 0.5]$ MeV, the probability $P \subset [0.04, 0.99]$ can be any sub-unitary value.

Conventionally, a barrier is parametrized as a function of a dimensionless parameter ε within three smoothed joined parabolas, the first barrier being labeled with A, the second with B, the first well with Roman digit I and the second with II as displayed in figure 3.

In a simplified picture, when only rotational excitations constructed on a β vibration in the second well are allowed, it can be considered that the energy widths for fission, neutron emission and gamma de-excitation are, respectively:

Table 1. Parameters of the phenomenological barrier.

V_A (MeV)	V_{II} (MeV)	V_B (MeV)	$\hbar\omega_A$ (MeV)	$\hbar\omega_{\mathrm{II}}$ (MeV)	$\hbar\omega_B$ (MeV)
6.1149	2.2759	6.198	0.64	0.95	0.715

$$\begin{aligned}\Gamma_f(J,E^*) &= \frac{1}{2\pi\rho(J,E^*,A)C_J}\\ &\times \sum\nolimits_{\Omega=1/2}^{J}\sum\nolimits_{L=0}^{J-\Omega}\langle jL\Omega 0|J\Omega\rangle^2\\ &\times \int_0^{E^*-E_0(L,\Omega)} T_{f,L,\Omega}(E)\rho(j,E^*-E_0(L,\Omega)-E,A)\,dE,\end{aligned} \tag{2}$$

$$\begin{aligned}\Gamma_n(J,E^*) &= \frac{1}{2\pi\rho(J,E^*,A)C_J}\\ &\times \sum_{\Omega=1/2}^{J}\sum_{L=0}^{J-\Omega}\sum_{l=0}^{l_m}\frac{\langle jL\Omega 0|J\Omega\rangle^2}{(l_m+1)}\\ &\times \int_0^{E_n-E_0(L,\Omega)}\frac{1}{2}T_{n,l}[\rho(j-1/2,E_n-E_0(L,\Omega),A-1)\\ &+\rho(j+1/2,E_n-E_0(L,\Omega),A-1)]\,dE,\end{aligned} \tag{3}$$

$$\begin{aligned}\Gamma_\gamma(J,E^*) &= \frac{1}{2\pi\rho(J,E^*,A)C_J}\\ &\times \sum_{\Omega=1/2}^{J}\sum_{L=0}^{J-\Omega}\langle jL\Omega 0|J\Omega\rangle^2\sum_{j'=|j-1|}^{j+1}\\ &\times \int_0^{E^*-E_0(L,\Omega)} C_\gamma A^{2/3}E^3\rho(j,E^*-E_0(L,\Omega)-E,A)\,dE,\end{aligned} \tag{4}$$

where

$$C_J = \sum_{\Omega=1/2}^{J}\sum_{L=0}^{J-\Omega}\langle jL\Omega 0|J\Omega\rangle^2 \tag{5}$$

is a normalization constant, T are transmissions, $C_\gamma = 2 \times 10^{-9}$, E_0 is the energy lost by the compound nucleus to produce the rotational collective motion, l_m is the maximal orbital momentum carried by the neutron (3 in this work), E^* is the excitation energy of the compound nucleus.

In the previous formulas, it is considered that a state (J, Ω) is unfolded under the states (j, Ω, L) through Clebsh-Gordon coefficients. Each of these states is characterized by its own transmission. J is the spin of the compound nucleus and Ω its projection on the symmetry axis, while j is the spin of the core that rotates with an angular momentum L. The barriers of the discrete transition states of the rotational levels are obtained by adding the excitations energies

$$\begin{aligned}E_x(L,\Omega) &= \frac{\hbar^2}{2J_x}[L(L+2\Omega+1)\\ &\quad + a(-1)^{J+1/2}(J+1/2)\delta_{\Omega,1/2}] - E_0(L,\Omega),\\ E_0(L,\Omega) &= \frac{\hbar^2}{2J_{\mathrm{I}}}[L(L+2\Omega+1)\\ &\quad + a(-1)^{J+1/2}(J+1/2)\delta_{\Omega,1/2}],\end{aligned} \tag{6}$$

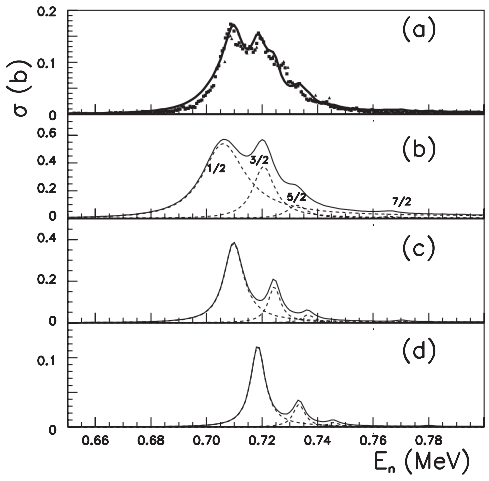

Fig. 4. Structure of the 0.7 MeV resonance. (a) Theoretical curve (full line) compared with experimental data from refs. [2] (squares) and [4] (triangles). This curve is the weighted sum of three fission cross sections. (b) Fission cross-section calculated for the parametrized barrier without excitation. The spin components of the cross section are labeled. (c) Fission cross section due to the first excitation. (d) Fission cross section due to the second excitation.

where $x = \mathrm{I}, \mathrm{II}, A, B$, are the extrema of the parametrized barrier, J_x is the moment of inertia and a is the decoupling parameter. If a certain level $\Omega = 1/2$ of low excitation energy carries the fission strength, then

$$\int_0^{E^*-E_0(L,\Omega)} T_{f,L,\Omega}(E)\rho(j, E^* - E_0(L,\Omega) - E, A)dE \approx T_{f,L,\Omega}[E_\Omega - E_0(L,\Omega)], \quad (7)$$

where E_Ω is the initial energy of the transition level Ω. Moreover, if the transition level is split in N different levels due to the radial coupling in the region of the second barrier, the transmission becomes:

$$T_{f,L,\Omega}[E_\Omega - E_0(L,\Omega)] = \sum_{i=1}^{N} p_i T_{f,L,\Omega,i}[E_\Omega - E_0(L,\Omega)], \quad (8)$$

where p_i denotes the probability that the single particle energy path i that creates a transition level with the transmission T_i is followed by the nuclear system. The number of different levels is $N = 3$ as indicated by the theoretical calculations. Finally, the fission cross section within the previous ingredients is:

$$\sigma_f(E^*) = \sum_J \sigma_C(J, E^*) \frac{\Gamma_f(J, E^*)}{\Gamma_f(J, E^*) + \Gamma_\gamma(J, E^*) + \Gamma_n(J, E^*)}, \quad (9)$$

where $\sigma_C(J, E^*)$ represents the compound nucleus cross section.

Using a value of the decoupling parameter $a = 0.8$, two excitations of 0.45 and 0.74 MeV produced with the probabilities 0.295 and 0.610, respectively, and using the parameters of the phenomenologic barrier given in table 1, a structure that agrees well with experimental data was obtained. This structure is plotted in figure 4 and compared with experimental data.

4 Conclusions

The scope of the present work is to understand the mechanism for the formation of the fission cross section structure and of the high number of resonances appealing essentially to dynamical single-particle effects associated to β-vibration in the second well. The number of free parameters is kept as minimal as possible to show evidence of the physics of the problem.

Theoretical excitations and their associated probabilities were determined theoretically for a given partition in the isotopic distribution of fragments. These excitations are added to a phenomenological barrier in the framework of the hybrid model. After the suitable search of the parameters of the double humped phenomenological barrier, the cross section is computed. The results give a rather good qualitative agreement with experimental data.

A way to introduce this new mechanism in the simulation of the structure of the cross section is evidenced.

The present investigation shows that the resonant structure of the fission cross section can be explained by the existence of many barriers associated to single-particle excitations. So, it is possible that the complex structure in the fission cross section is due to rearrangement of orbitals and the dynamic of the process, beginning from the initial state of the compound nucleus and terminating at the scission. A large number of different excited barriers are formed leading to a large number of vibrational resonances in the second well. These resonances carry information about the structure of the nucleus at hyper-deformations and the dynamics. The model presented in this work represents an alternative to the actual statistical models and may determine a competitive way to consider the fission process.

References

1. G.D. James, J.E. Lynn, L.G. Earkwaker, Nucl. Phys. A **189**, 225 (1972).
2. J. Blons, C. Mazur, D. Paya, M. Ribrag, H. Weigmann, Phys. Rev. Lett. **41**, 1289 (1978).
3. A. Sicre, T. Benfoughal, B. Bruneau, M. Asghar, G. Barreau, F. Caitucoli, T.P. Doan, G.D. James, B. Leroux, Nucl. Phys. A **445**, 37 (1985).
4. J.W. Boldeman, R.L. Walsh, *Proceedings of the International Conference Nuclear Data for Basic and Applied Science, Santa Fe, New Mexico, 13–17 May 1985*, P.G. Young, R.E. Brown, G.F. Auchampaugh, P.W. Lisowski, L. Steward (eds.) (Gordon and Breach Science Publishers, NY), pp. 317–322.
5. M. Mirea, L. Tassangot, C. Stephan, C.O. Bacri, P. Stoica, R.C. Bobulescu, J. Phys. G **31**, 1165 (2005).
6. M. Mirea, Nucl. Phys. A **780**, 13 (2006).
7. M. Mirea, L. Tassangot, C. Stephan, C.O. Bacri, R.C. Bobulescu, Europhys. Lett. **73**, 705 (2006).
8. W. Greiner, J.Y. Park, W. Scheid, in *Nuclear Molecules* (World Scientific, Singapore, 1995), Ch. 11.
9. M. Mirea, Phys. Rev. C **63**, 034603 (2001).
10. http://www.nndc.bnl.gov/index.jsp.